

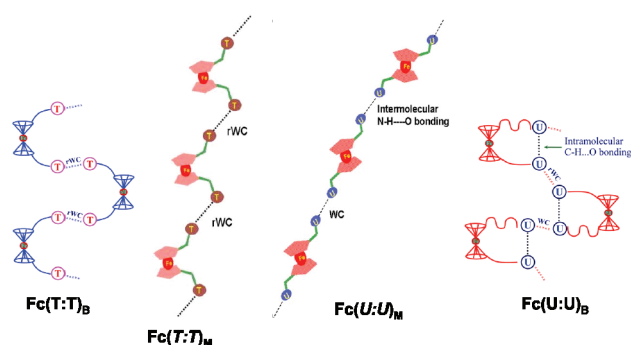
Ferrocene–Bis(thymine/uracil) Conjugates: Base Pairing Directed, Spacer Dependent Self-Assembly and Supramolecular Packing

Amit N. Patwa,[†] Rajesh G. Gonnade,[‡] Vaijayanti A. Kumar,[†] Mohan M. Bhadbhade,[‡] and Krishna N. Ganesh^{*†,§}

[†]Division of Organic Chemistry, and [‡]Center For Materials Characterization, National Chemical Laboratory, Pune 411008, India, and [§]Indian Institute of Science Education and Research, 900, NCL Innovation Park, Dr Homi Bhabha Road, Pune 411008, India

kn.ganesh@iiserpune.ac.in

Received September 27, 2010



Base pairing Fc-(Thymine/Uracil) conjugates with different spacer chain

X-ray crystallographic studies of methylene linked Ferrocene-bis(thymine/uracil) conjugates $\text{Fc}(\text{T:T})_{\text{M}}$ and $\text{Fc}(\text{U:U})_{\text{M}}$ reveal base dependent 2-D supramolecular assemblies generated via wobble self-pairing for bis-thymine and reverse wobble self-pairing for bis-uracil conjugates, differing in architecture from the corresponding butylene spacer linked conjugates

Development of supramolecular assemblies¹ into well-defined architectures has been a subject of great interest in recent years in view of its importance in understanding principles of molecular recognition and the associated structural features of biomolecules such as proteins, lipids, and nucleic acids that are important for self-organization. A system of evolutionary perfection for molecular self-assembly is DNA/RNA.² The hydrogen bond mediated supramolecular interactions found in nucleic acids have provided inspiration to design a number of

novel self-assembling systems.^{3,4} In recent years, bio-organometallic chemistry has grown rapidly, networking the classical organometallic chemistry to biology and molecular biotechnology.^{3,5} The redox active ferrocene unit linked to self-base pairing nucleobases⁶ or DNA/RNA could be a useful building block in supramolecular chemistry. When coupled to molecular recognition and electrochemistry, this may lead to electrochemical recognition of DNA/RNA binding substrates.⁵ Recently we have reported⁷ a study on ferrocenyl mono- and bis(thymine/uracil) conjugates with an *n*-butyl spacer [$\text{Fc}(\text{T:T})_{\text{B}}$, $\text{Fc}(\text{U:U})_{\text{B}}$] whose crystal structures exhibited base pair induced self-assembly leading to novel supramolecular packing. The structure of $\text{Fc}(\text{U:U})_{\text{B}}$ is perhaps the first example wherein both wobble and reverse wobble self-pairings are simultaneously present within the same crystal lattice. The 5-substituent (H, Me, Br) on the pyrimidine base seems to sterically influence the supramolecular packing by inhibiting specific intermolecular C–H···O contacts as seen in the structure of $\text{Fe}(5\text{-BrU:5-BrU})_{\text{B}}$ and the chimeric $\text{Fe}(\text{T:U})_{\text{B}}$. The base pairing directed contiguous self-assemblies are seen only in bis substituted ferrocene conjugates and as expected are absent in mono T/U substituted ferrocene conjugates. Ferrocene type scaffolds have also utility in inducing chain reversal⁸ in peptides.

The same butyl (C4) spacer chain induced different packing in the two conjugates, and in $\text{Fc}(\text{U:U})_{\text{B}}$ even the two spacers in the same molecule have different conformations. In order to examine the role of spacer chain in directing the base pairing and molecular packing, herein we present synthesis and studies on self-assembling properties of ferrocenyl bis-thymine and bis-uracil conjugates (**5a–b**) having a C1 methylene spacer [$\text{Fe}(\text{T:T})_{\text{M}}$ and $\text{Fe}(\text{U:U})_{\text{M}}$] (Figure 1), which was chosen because of ease of synthesis. It is seen that the replacement of C4 butyl chain spacer with C1 methylene spacer still results in self-pairing but has different consequences in T and U conjugates in directing the self-assembly and molecular packing in crystals.

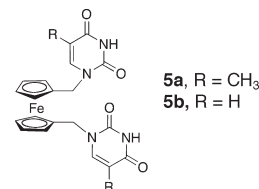


FIGURE 1. Ferrocene linked thymine/uracil conjugates with methylene spacer **5a** $\text{Fe}(\text{T:T})_{\text{M}}$ and **5b** $\text{Fe}(\text{U:U})_{\text{M}}$.

1,1'-Ferrocene dicarbaldehyde **2** (Scheme 1) was synthesized from ferrocene **1** in good yield by treating the dilithioferrocene–TMEDA complex with dimethylformamide (DMF).⁹

(1) (a) Steed, J. W.; Atwood, J. L. *Supramolecular Chemistry*; Wiley: Chichester, 2000. (b) Lehn, J.-M. *Supramolecular Chemistry—Concepts and Perspectives*; VCH: Weinheim, 1995; Chapter 9.

(2) (a) Saenger, W. *Principles of Nucleic Acid Structure*; Springer-Verlag: New York, 1984. (b) Leonard, G. A.; Zhang, S.; Peterson, M. R.; Harrop, S. J.; Helliwell, J. R.; Cruse, W. B.; d'Estaintot, B. L.; Kennard, O.; Brown, T.; Hunter, W. N. *Structure* **1995**, *3*, 335–340.

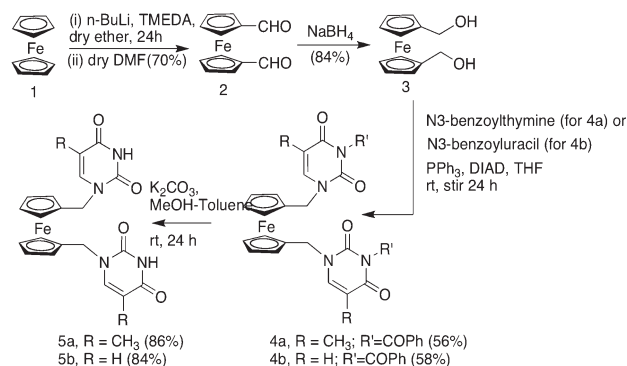
(3) Cooke, G.; Rotello, V. M. *Chem. Soc. Rev.* **2002**, *31*, 275–286.

(4) (a) Sivakova, S.; Rowan, S. J. *Chem. Soc. Rev.* **2005**, *34*, 9–21. (b) Davis, J. T. *Angew. Chem., Int. Ed.* **2004**, *43*, 668–698. (c) White, C. M.; Gonzalez, M. F.; Bradwell, D. A.; Rees, L. H.; Jeffrey, J.; Ward, M. D.; Armadori, N.; Calogero, G.; Barigelletti, F. *J. Chem. Soc., Dalton Trans.* **1997**, 727–735.

(5) (a) Schlotter, K.; Boeckler, F.; Hübner, H.; Gmeiner, P. *J. Med. Chem.* **2005**, *48*, 3696–3699. (b) Van Staveren, D. R.; Metzler-Nolte, N. *Chem. Rev.* **2004**, *104*, 5931–5986. and references therein. (c) Kumar, J.; Purohit, C. S.; Verma, S. *Chem. Commun.* **2008**, 2526–2528.

(6) Houlton, A.; Isaac, C. J.; Gibson, A. E.; Horrocks, B. R.; Clegg, W.; Elsegood, M. R. J. *J. Chem. Soc., Dalton Trans.* **1999**, 3229–3234.

(7) Patwa, A. N.; Gupta, S.; Gonnade, R. G.; Kumar, V. A.; Bhadbhade, M. M.; Ganesh, K. N. *J. Org. Chem.* **2008**, *73*, 1508–1515.

SCHEME 1. Synthesis of Compounds 5a and 5b^a

^aValues in brackets in each step indicate yields.

Compound **2** on reduction with NaBH₄ gave the diol 1,1'-bis(hydroxymethyl)ferrocene **3** that was reacted with *N*3-benzoylthymine/*N*3-benzoyluracil, under Mitsunobu reaction conditions to yield the conjugates **4a,b**. *N*-Debenzoylation of **4a,b** with aq K₂CO₃ in methanol/toluene gave the target compounds **5a,b**. All compounds were characterized by ¹H NMR and mass spectral data (see Supporting Information).

Crystallization. Slow evaporation of Fc(T:T)_M **5a** and Fc(U:U)_M **5b** in dichloromethane/methanol solution produced yellow colored single crystals. The crystals of Fc(T:T)_M **5a** belong to the monoclinic unit cell in the *P*2₁/*n* space group, whereas Fc(U:U)_M **5b** showed monoclinic unit cell in the *P*2₁/*c* space group.

X-ray Crystal Structures of Fc(T:T)_M and Fc(U:U)_M **5a,b**.

In Fc(T:T)_M **5a**, the two-cyclopentadienyl (Cp) rings of the ferrocene moiety are almost eclipsed (staggered by ~4°) and both methylene spacers linked with thymines are in extended conformation on the same lateral side (*cis*) of ferrocene but projecting on the opposite faces of the Cp rings (Figure 2A). The thymine bases are almost perpendicular in orientation to Cp ring with a torsion twist of ~108° about the linker methylene carbon, and the methyl groups attached to C5 atoms of the two thymine bases point away from each other. The centroid–centroid separation of the Cp rings is 3.298(2) Å with a dihedral angle of 5.43°, and the Cp–Fe–Cp angle is 174.89(7)°.

In contrast, the uracil analogue Fc(U:U)_M **5b** has nucleobases on opposite sides (*trans*) of the ferrocenyl moiety with two cyclopentadienyl (Cp) rings staggered by ~19° (Figure 2B). Similar to **5a**, the methylene spacers linking uracil to ferrocene adopt an extended conformation and the uracils adopt a torsion twist of ~112° about the methylene carbon. The centroid–centroid separation of the Cp rings is 3.294(3) Å with a dihedral angle of 1.35°, and the Cp–Fe–Cp angle is 178.96(11)°.

Base Pairing. The neighboring molecules in Fc(T:T)_M **5a** exhibit self-base pairing *via* two conventional N2A–H2NA···O1 and N2–H2N···O1A hydrogen bonds comprising “reverse” wobble pairing (Figure 3A). The thymine at C1 of Cp is engaged in hydrogen bond formation with the other thymine substituted at C1A of Cp of the unit-translated molecule along the 010 axis, creating pseudocentrosymmetric dimers. The geometry of intermolecular H-bonds in the base pairing indicated that the geometry of one of the H-bonds of the reverse

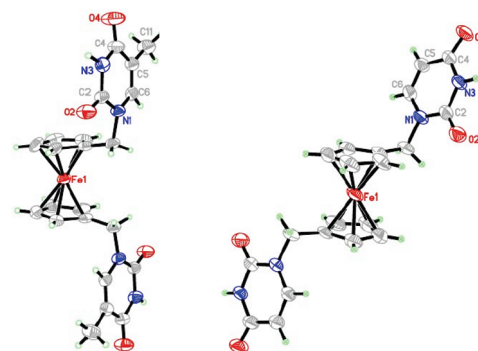


FIGURE 2. ORTEP of Fc(T:T)_M **5a** (A) and Fc(U:U)_M **5b** (B).

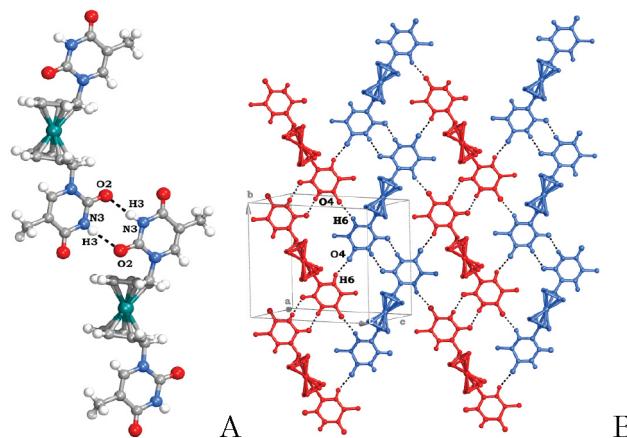


FIGURE 3. (A) N–H···O linked molecules ribbon (blue and red) formed through contiguous self-base pairing of reverse wobble type in Fc(T:T)_M **5a**. (B) Association of the two ribbons *via* C–H···O contacts forming sheet in 2D in Fc(T:T)_M **5a**.

wobble base pair (H3NA···O2) is slightly better compared to the other (H3N···O2A) (Table 1)

Interestingly, in the bis-uracil derivative Fc(U:U)_M **5b**, only one U attached to the ferrocene unit is engaged in wobble self-base pairing *via* conventional centrosymmetric N3–H3N···O4 hydrogen bonding (Figure 4, light pink strip) while the other U is nonpaired (Figure 4, cyan strip). This unpaired U links the adjacent centrosymmetric base pairs *via* N–H···O hydrogen bond along the *b*-axis.

Molecular Packing and Role of Spacer Chain. The adjacent ribbons in Fc(T:T)_M **5a** (Figure 3B), each formed by a contiguous self-pairing motif as a dominant synthon, are related by *n*-glide symmetry and stitched together *via* strong C–H···O hydrogen bonds (see Table 1, Supporting Information). The C6–H6 of thymine at C1 of Cp forms an almost linear C–H···O hydrogen bond with the carbonyl oxygen O4 of thymine at C1A of Cp. In turn, the C5–CHA of thymine at C1A forms short and linear hydrogen bond with the carbonyl oxygen O2 of thymine at C1. This leads to a two-dimensional sheet that extends within the 101 plane with all ferrocene moieties remaining on one side of the sheet (Figure 3B). These sheets are further linked centrosymmetrically to another parallel sheet with the assistance of two weak C–H···O hydrogen bonds engaging carbonyl oxygens (O2 and O4) and both methyl groups (C5 and C5A) of thymine (C5–CH₃···O4 and C5A–CH₃···O4A). This creates a channel embedding ferrocene moieties in close proximity *via* weak van der Waal’s interactions (Figure 5A).

(8) Moriuchi, T.; Nagai, T.; Hirao, T. *Org. Lett.* **2006**, *8*, 31–34.

(9) Balavoine, G. G. A.; Doisneau, G.; Filleben-Khan, T. J. *Organomet. Chem.* **1991**, *412*, 381–382.

TABLE 1. Intermolecular H-Bonding Geometry

		D–H...A	H...A (Å)	D...A (Å)	D–H...A (deg)
base pairing	5a	D–H...A	1.99	2.847(3)	174.9
		N3A–H3NA...O2	2.03	2.869(3)	164.9
	5b	N3A–H3NA...O4	2.01	2.853(4)	165.0
		N2–H2N...O4A	1.96	2.807(4)	170.0

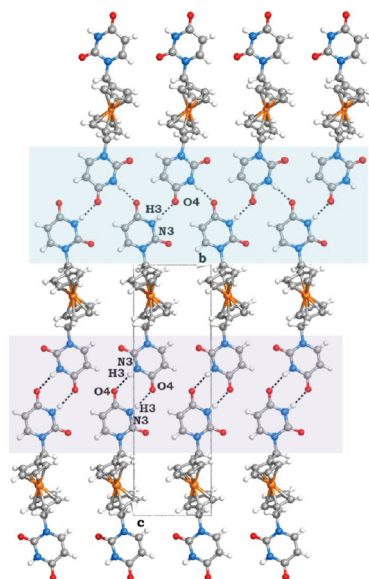


FIGURE 4. Wobble type self-base pairs *via* centrosymmetric N–H...O hydrogen bonds (highlighted in cyan) connected through catemeric N–H...O hydrogen bond (shaded in light pink) in Fc(U:U)_M **5b**.

In the case of Fc(U:U)_M **5b**, the carbonyl oxygen O4A participating in wobble motif (N3A–H3NA) is involved in centrosymmetric hydrogen bonding *via* C5A–H5A...O4A interactions with adjacent chain. The carbonyl oxygen O2A of uracil is also centrosymmetrically bonded *via* C–H...O interactions to C6A–H6A of neighboring chain (Figure 4). These two C–H...O interactions connect the two wobble type base pairs with formation of a tetrad with the help of N2A–H, C5A–H, and C6A–H sites as hydrogen bond donors and O2A, O4A acting as hydrogen bond acceptors. The four uracil moieties connected to each other form a quartet structure *via* centrosymmetric N–H...O and C–H...O interactions. Linking of the uracil moieties on both sides of ferrocene generates a continuous sheet formation in 2-dimensional space. The adjacent sheets along the *b*-axis are linked *via* π – π stacking interactions between the substituted Cp rings of ferrocene as well as between the uracil moiety and the neighboring sheets are bound by a weak C–H...O interaction from CpC4A–H4A...O4A (Figure 5B). The crystal data of **5b** are given in Supporting Information.

In comparison with the earlier results on butyl C4 spacer chain, the present crystal structures of Fc(T:T)_M **5a** and Fc(U:U)_M **5b** with C1 spacer chains clearly indicate the role of the linker chain in directing the self-assembly induced supramolecular structure. The identical folding of two butyl chains in Fc(T:T)_B is different from the unsymmetrical pattern in Fc(U:U)_B suggesting some flexibility, and the C1 spacer gives a more rigid packing in **5a** and **5b**. The intermolecular packing seems to be a consequence of optimized π – π stacking and C–H...O interactions to the extent that the bases are forced to

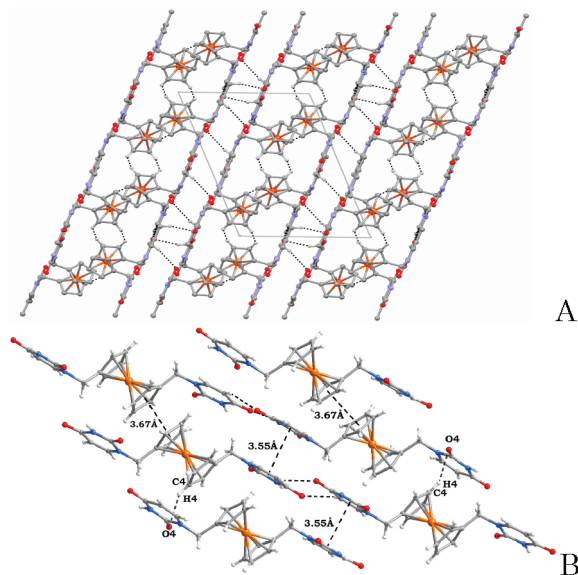


FIGURE 5. (A) Molecular packing diagram of Fc(T:T)_M **5a** viewed down the *b*-axis. (B) Perpendicular view of the sheets in Fc(U:U)_M **5b**. Adjacent sheets associate *via* π – π and C–H...O interactions.

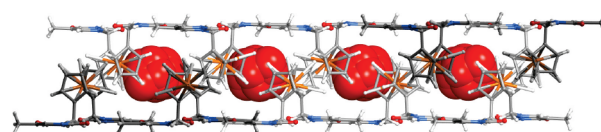


FIGURE 6. Disordered water molecules trapped in ferrocene cage in Fc(T:T)_M formed by contiguous self-pairing of thymines.

assume *cis* disposition with respect to ferrocene unit in Fc(T:T)_M and *trans* in Fc(U:U)_M. The association of neighboring sheets through C–H...O bonds differs among these leading to different supramolecular architecture.

In both C4 and C1 spacer linked Fc(T:T)_{M/B}, a contiguous intermolecular self-pairing of thymines leads to a regular ribbon formation. In the case of Fc(U:U)_M, self-base pairing was restricted to the dimer level without any contiguity to form a strip unlike Fc(U:U)_B. Interestingly, in Fc(T:T)_M four disordered water molecules are trapped in the cage formed by the self-assembly process, with no significant interactions between the host and the guest molecules (Figure 6). This seems to be a consequence of not only the ferrocene cage structure seen specifically in Fc(T:T)_M but also a compact hydrophobic pocket created by the four methyl groups of self-paired thymines. This was not seen in case of Fc(T:T)_B having a longer butyl spacer chain between ferrocene and thymine.

In conclusion, the crystal structure results on ferrocene–nucleobase conjugates Fc(T:T)_M and Fc(U:U)_M with short methylene spacer chains indicate pyrimidine base dependent self-base pairing *via* a reverse wobble type for T and a wobble type for U bases. While contiguous base pairs in Fc(T:T) with both methylene and butyl spacers lead to formation of

tape structures, held together by C–H···O bonds, Fc(U:U) base pairs lead to a chain formed by alternative self-base pairing and C–H···O bonding. Extensive π – π stacking is seen in both cases leading to different patterns of molecular packing. The nature of the spacer (methylene vs butyl) has an effect on the 3D molecular packing in the crystals and relative orientation of Cp rings in different conjugates. Hydrophobic cavities created in Fc(T:T)_M **5a** even lead to trapping of water molecules. The accurate geometries of the T:T and U:U self-base pairs seen in Fc(T:T)_{M/B} and Fc(U:U)_{M/B} is of considerable interest due to their structural relevance to nucleic acids. Similar work in analysis of geometry of hetero base pairs in Fc(A:T) and Fc(A:U) and electrochemical studies is in progress.

Experimental Section

For general experimental conditions and spectra, see Supporting Information.

1,1'-Bis(hydroxymethylene)ferrocene 3. 1,1'-Ferrocene carboxaldehyde **2**⁸ (1.55 g, 6.4 mmol) in methanol (25 mL) was stirred at 0 °C for 10 min, and NaBH₄ (0.54 g, 14.1 mmol) was added portionwise, keeping the temperature below 0 °C. The reaction mixture was stirred for 1 h at room temperature. The solvent was removed under reduced pressure, and the residual material was extracted with ethyl acetate (3 × 75 mL). The combined organic phase on workup gave crude product that was purified by silica gel chromatography to give **3** recrystallized from ethyl acetate/petroleum ether to give **3** as yellow needles. Yield 84%; mp 106–108 °C; ¹H NMR (CDCl₃, 200 MHz) δ 3.54 (s, 2H), 4.19 (s, 4H), 4.22 (s, 4H), 4.40 (s, 4H); ¹³C NMR (CDCl₃, 50 MHz) δ 60.2, 66.9, 67.9, 89.3; MS (LC–MS) (*m/z*) calcd for C₁₂H₁₄O₂Fe 246.08 [M⁺], found 246.08 [M⁺]. Anal. Calcd for C₁₂H₁₄O₂Fe: C, 58.57; H, 5.73. Found: C, 58.49; H, 5.81.

General Procedure for the Preparation of 4a and 4b via Mitsunobu Reaction. *N*3-Benzoylthymine/*N*3-benzoyluracil (3.75 mmol) and triphenylphosphine (1.18 g, 4.5 mmol) were dissolved in dry THF (25 mL), and the solution was cooled to 0 °C. At this temperature alcohol **3** (0.37 g, 1.5 mmol), dissolved in dry THF (10 mL), was added to the stirred solution followed by dropwise addition of DIAD (0.9 mL, 4.5 mmol). The solution was allowed to gradually reach room temperature, and stirring was continued overnight. The solvent was removed under reduced pressure, and the resulting solid was purified by flash chromatography on silica gel and elution with petroleum ether/ethyl acetate (1:1) to give ferrocene-linked *N*3-benzoylprotected nucleobases **4a** and **4b**.

1,1'-Bis(*N*3-benzoylthymine)methylene)ferrocene 4a. Yellow needle; yield 56%; mp 146–148 °C (DCM); IR (nujol) 1741, 1697, 1651 cm⁻¹; ¹H NMR (CDCl₃, 500 MHz) δ 1.91 (s, 6H), 4.23 (s, 4H), 4.28 (s, 4H), 4.66 (s, 4H), 7.07 (s, 2H), 7.45–7.53 (m, 4H), 7.61–7.70 (m, 2H), 7.89–7.94 (m, 4H); ¹³C NMR (CDCl₃, 125 MHz) δ 12.4, 14.2, 47.1, 69.8, 82.3, 110.9, 129.1, 130.4, 131.6, 135.0, 139.2, 149.9, 162.9, 169.1; MS (LC–MS) (*m/z*) calcd for C₃₆H₃₀N₄O₆Fe 670.50 [M⁺], found 670.14 [M⁺]. Anal. Calcd for

C₃₆H₃₀N₄O₆Fe: C, 64.49; H, 4.51; N, 8.35. Found: C, 64.41; H, 4.63; N, 8.29.

1,1'-Bis(*N*3-benzoyluracilmethylene)ferrocene 4b. Yellow needle; Yield 58%; mp 223–225 °C (melt and decomp) (DCM); IR (nujol) 1745, 1699, 1651 cm⁻¹; ¹H NMR (CDCl₃, 500 MHz) δ 4.25 (s, 4H), 4.28 (s, 4H), 4.68 (s, 4H), 5.75 (d, 2H, *J* = 8.3 Hz), 7.22 (d, 2H, *J* = 7.8 Hz), 7.48–7.52 (m, 4H), 7.64–7.67 (m, 2H), 7.91–7.93 (m, 4H); ¹³C NMR (CDCl₃, 125 MHz) δ 47.4, 70.4, 81.9, 102.3, 129.2, 130.5, 131.4, 135.2, 143.1, 149.9, 162.2, 168.8; MS (LC–MS) (*m/z*) calcd for C₃₄H₂₆N₄O₆Fe 642.45 [M⁺], found 642.03 [M⁺]. Anal. Calcd for C₃₄H₂₆N₄O₆Fe: C, 63.56; H, 4.08; N, 8.72. Found: C, 63.39; H, 4.21; N, 8.66.

General Procedure of Benzoylation for the Preparation of 5a and 5b. To a stirred solution of dibenzoyl derivative of **4a** and **4b** (0.3 mmol) in a THF/MeOH/H₂O mixture (1:1:0.05, 100 mL) was added K₂CO₃ (0.34 g, 2.4 mmol). The resultant mixture was then stirred at room temperature overnight. The solvent was removed under reduced pressure/ and the residual material was extracted with dichloromethane/methanol (30:1, 3 × 50 mL). The combined organic phase was washed with brine solution, dried over Na₂SO₄, and concentrated to give crude ferrocene-linked nucleobases **5a** and **5b**. The crude products were recrystallized from the appropriate solvent.

1,1'-Bis(thymine)methylene)ferrocene 5a. Yellow needle; yield 86%; mp 250 °C (decomp) (DCM/MeOH); IR (nujol) 3153, 1681, 1668 cm⁻¹; ¹H NMR (DMSO-*d*₆, 500 MHz) δ 1.77 (s, 6H), 4.42 (s, 4H), 4.37 (s, 4H), 4.61 (s, 4H), 7.61 (s, 2H); ¹³C NMR (DMSO-*d*₆, 125 MHz) δ 12.2, 46.1, 69.2, 69.8, 83.7, 108.8, 141.0, 151.1, 164.6; MS (LC–MS) (*m/z*) calcd for C₂₂H₂₂N₄O₄Fe 462.52 [M⁺], found 485.00 [M⁺ + Na]. Anal. Calcd for C₂₂H₂₂N₄O₄Fe: C, 57.13; H, 4.79; N, 12.11. Found: C, 57.33; H, 4.92; N, 12.23.

1,1'-Bis(uracilmethylene)ferrocene 5b. Yellow flakes; yield 84%; mp 260 °C (decomp) (DCM/MeOH); IR (nujol) 3138, 1697, 1658 cm⁻¹; ¹H NMR (DMSO-*d*₆, 500 MHz) δ 4.23 (s, 4H), 4.37 (s, 4H), 4.65 (s, 4H), 5.58 (d, 2H, *J* = 7.8 Hz), 7.74 (d, 2H, *J* = 7.8 Hz), 11.28 (br s, 2H); ¹³C NMR (DMSO-*d*₆, 125 MHz) δ 46.4, 69.3, 69.8, 83.6, 101.2, 145.4, 151.0, 163.9; MS (LC–MS) (*m/z*) calcd for C₂₀H₁₈N₄O₄Fe 434.23 [M⁺], found 434.30 [M⁺]. Anal. Calcd for C₂₀H₁₈N₄O₄Fe: C, 55.32; H, 4.18; N, 12.90. Found: C, 55.45; H, 4.32; N, 12.77.

Acknowledgment. A.N.P. thanks CSIR, New Delhi for a research fellowship, and K.N.G. is a JC Bose Fellow of Department of Science and Technology, New Delhi. We acknowledge Mayura Talwalekar for partial assistance in X-ray work.

Supporting Information Available: Experimental procedures and spectral data for all new compounds and crystallographic data of **5a,b** in CIF format. This material is available free of charge via the Internet at <http://pubs.acs.org>.